On the other hand, integration of eq 24, taking eq 27 and 29 into account, classically[22] leads to eq 5, noting that ξ and τ are related by means of the linear relationship between the electrode potential and time, $E = E_i - vt$ (E_i = starting potential of the scan). Thus $\xi + u = \tau$, where $u = (F/RT)(E_i - E^R{}_1)$ is a dimensionless measure of the starting potential referred to the reduction potential $E^R{}_1$. In practice, $u = \infty$, meaning that the scan is started at a potential sufficiently positive to the waves for them to be independent of its exact value.

When going to preparative-scale conditions, eq 24-26 become ordinary differential equations since the time derivatives are now zero. Space is now normalized toward the thickness, δ, of the steady-state diffusion layer,[17,22] i.e., $y = x/\delta$. Accordingly, the currents are normalized toward the diffusion current i_l (see eq 14 and 15 in the text). There are two sets of boundary conditions, one for the electrode surface ($y = 0$) which is formally the same as above (eq 28-30) and the other at the edge of the diffusion layer ($y = 1$) which is the same as eq 27. Integration, again taking into account the fact that, reaction 3 being rapid, $R^\bullet$ only exists in a thin reaction layer within the diffusion layer, immediately leads to eq 13 and 6. When the potential becomes more and more negative ($\xi \rightarrow \infty$), both Ψ_1 and $\Psi_2 \rightarrow 1$. The half-wave potential of the second wave, E^l, thus corresponds to $\Psi_2 = 0.5$. Application of eq 6 to this particular condition thus leads to eq 19.

In the linearization of the quadratic kinetic law:

$$\Delta G^\ddagger = \Delta G^\ddagger{}_0\left(1 + \frac{E - E^0 - \Phi_r}{4\Delta G^\ddagger{}_0}\right)^2 \tag{35}$$

the transfer coefficient:

$$\alpha = \frac{1}{2}\left(1 + \frac{E - E^0 - \Phi_r}{4\Delta G^\ddagger{}_0}\right) \tag{36}$$

is regarded as constant and equal to its value at the peak:

$$\alpha = \frac{1}{2}\left(1 + \frac{E^p - E^0 - \Phi_r}{4\Delta G^\ddagger{}_0}\right) \tag{37}$$

Accordingly, the electrode potential is regarded as undergoing only small variations around the peak potential: $E = E^p + \Delta E$. Equation 35 can thus be linearized as:

$$\Delta G^\ddagger = \Delta G^\ddagger{}_0\left[\left(1 + \frac{E^p - E^0 - \Phi_r}{4\Delta G^\ddagger{}_0}\right)^2 + \frac{\Delta E}{2\Delta G^\ddagger{}_0}\left(1 + \frac{E^p - E^0 - \Phi_r}{4\Delta G^\ddagger{}_0}\right)\right] \tag{38}$$

i.e.,

$$\Delta G^\ddagger = 4\alpha(1 - \alpha)\Delta G^\ddagger{}_0 + \alpha(E - E^\circ - \Phi_r) \tag{39}$$

Since

$$\Delta G^\ddagger = \frac{RT}{F}\ln\frac{Z^{el}}{k^f} + \alpha E \tag{40}$$

(Z^{el} is the heterogeneous collision frequency), it follows that:

$$\frac{RT}{F}\ln\frac{Z^{el}}{k^f} = 4\alpha(1 - \alpha)\,\Delta G^\ddagger{}_0 - \alpha(E^0 - \Phi_r) \tag{41}$$

The final equations used in the text (eq 22 and 23) then result from linear combination of eq 37 and 41.

(22) Andrieux, C. P.; Savéant, J-M. Electrochemical Reactions. In *Investigations of Rates and Mechanisms of Reactions*; Bernasconi, C. F., Ed.; Techniques of Chemistry; Wiley: New York, 1986; Vol. 6, 4/E, Part 2, pp 305-390.

Protonation Dynamics of $[(C_5H_5)(CO)Fe]_2(\mu\text{-}CO)(\mu\text{-}C{=}CH_2)$ and Decomposition Processes for $[(C_5H_5)(CO)Fe]_2(\mu\text{-}CO)(\mu\text{-}C{=}CH_2)H^+$ in the Gas Phase

D. B. Jacobson

Contribution from the Department of Chemistry, North Dakota State University, Fargo, North Dakota 58105-5516. *Received April 28, 1988*

Abstract: The proton affinity (PA) and site of protonation of $[(C_5H_5)(CO)Fe]_2(\mu\text{-}CO)(\mu\text{-}C{=}CH_2)$ (**2**), as well as the decomposition processes for $[(C_5H_5)(CO)Fe]_2(\mu\text{-}CO)(\mu\text{-}C{=}CH_2)H^+$ (**7**), are studied in the gas phase by using Fourier transform mass spectrometry (FTMS). The PA of **2** is assigned as 232.5 ± 2 kcal/mol (relative to $PA(NH_3)$ = 204.0 kcal/mol) by using the bracketing technique. The site of protonation was determined by labeling studies to be the β-carbon of the μ-ethenylidene group of **2** yielding **3** in accord with the known solution chemistry. Protonation of **2** forming **3** implies that **3** is thermally more stable than isomeric μ-ethenyl species **6**. That both **3** and **6** have similar thermodynamic stability in solution implies that **6** is stabilized more by solvation than the corresponding μ-ethylidyne **3**. In contrast to solution, **3** is inert toward carbonyl electrophiles (aldehydes and ketones). This difference in reactivity, however, is consistent with the proposed reaction mechanism in solution involving initial protonation of the carbonyl species. The decomposition processes for collisionally activated **3** were studied in detail and compared with that for the non-protonated analogue $[(C_5H_5)(CO)Fe]_2(\mu\text{-}CO)(\mu\text{-}C{=}CH_2)^+$ (**13**). **3** decomposes by initial elimination of the three carbonyls followed by sequential C_2H_2 and H_2 eliminations yielding respectively $[(C_5H_5)Fe]_2H^+$ (**10**) and $Fe_2C_{10}H_9^+$. Hydrogen migration in the above fragment ions was investigated by monitoring H/D exchange with D_2 and ethene-d_4. No exchange occurs for any of the ions ($[(C_5H_5)(CO)Fe]_2(\mu\text{-}CO)(\mu\text{-}C{=}CH_2)H^+$ through $[(C_5H_5)Fe]_2H^+$) with D_2. With ethene-d_4, one H/D exchange is observed with $[(C_5H_5)Fe]_2H^+$ (**10**), with *no* exchange for any of the larger fragment ions. Observation of only one exchange for **10** indicates that the exchangeable hydrogen is not scrambling with the cyclopentadienyl ring hydrogens.

Hydrocarbyl-bridged dinuclear transition-metal complexes[1] are the focus of increasing attention since they may serve as models for catalytic reactions. μ-Alkylidene and μ-alkylidyne dinuclear complexes are of particular interest due to their relevance as models for important catalytic processes including the Fischer-Tropsch synthesis.[2] Cationic bridging alkylidyne-diiron complexes (**1**) have been the focus of recent studies owing to their ease of synthesis and thermal stability. Rosenblum and co-workers[3] first

(1) For a review see: Holton, J.; Lappert, M. F.; Pearce, R.; Yarrow, P. I. W. *Chem. Rev.* **1983**, *83*, 135 and references cited therein.

(2) For reviews on Fischer-Tropsch synthesis, see: (a) Herrman, W. A. *Angew. Chem., Int. Ed. Engl.* **1982**, *21*, 117. (b) Muetterties, E. L.; Stein, J. *Chem. Rev.* **1979**, *79*, 479. (c) Rofer-Depoorter, C. K. *Chem. Rev.* **1981**, *81*, 447. Biloen, P.; Sachtler, W. M. H. *Adv. Catal.* **1981**, *30*, 165.

0002-7863/89/1511-1626$01.50/0

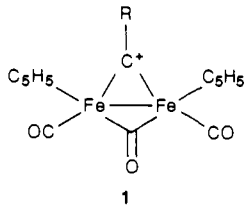

1

prepared these complexes (R = H) by reaction of RLi with $[(C_5H_5)(CO)Fe(\mu\text{-}CO)]_2$ followed by strong acid workup. Petit[4] and Stone[5] demonstrated that μ-ethenylidene complex (**2**) can be

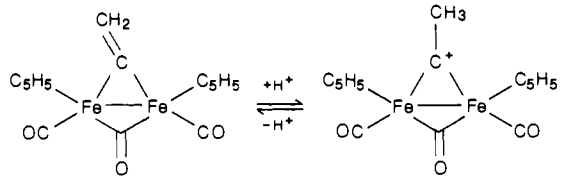

2 3

reversibly protonated yielding μ-ethylidyne **3**. Casey and coworkers[6] synthesized the bridging methylidyne complex (**4**) by hydride abstraction of the corresponding bridging methylidene complex (**5**), and represents the first example of a doubly bridging methylidyne complex.

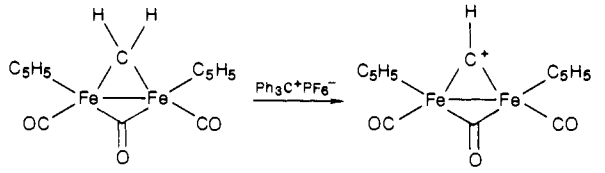

5 4

Two novel and important reactions have been observed for these μ-alkylidyne complexes. The first involves addition of the C–H bond of the μ-methylidyne in **4** across the C=C double bond of terminal alkenes forming new μ-alkylidyne species as exemplified by process 1.[7] This novel C–C bond formation process is the first

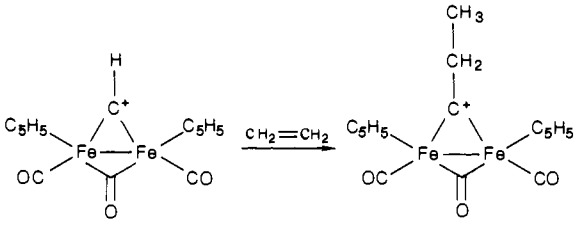

4 (1)

example of the addition of a C–H bond across the C=C double bond of simple alkenes and has been coined "hydrocarbation" by Casey.[8] The corresponding addition of a C-alkyl bond of an μ-alkylidyne complex across an alkene has not been observed.[8]

The other novel reaction involves the thermal rearrangement of cationic (μ-alkylidyne)diiron complexes to μ-alkenyl complexes via a 1,2-hydride shift, process 2.[9-11] The rate of the above rearrangement is very sensitive to the degree of substitution on

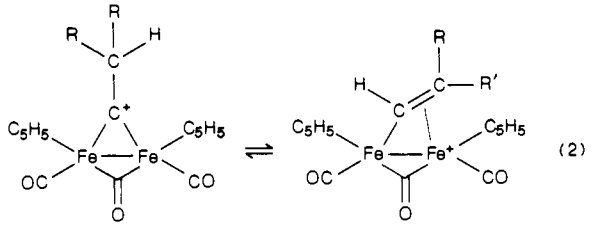

(2)

the β-carbon of the alkylidyne with increasing substitution facilitating this rearrangement.[10] For example, the bridging ethylidyne, **3**, does not isomerize to the corresponding ethenyl complex, **6**, upon heating to 88 °C in CD_2Cl_2 for 100 h.[3,4] The μ-ethenyl rearrangement product, **6**, was independently synthesized

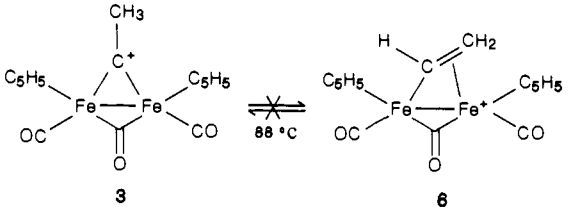

3 6

by hydride abstraction from a μ-ethylidene and found not to rearrange to **3** upon heating to 88 °C in CD_2Cl_2 for 20 h.[10] Casey has pointed out that the above trends suggest a buildup of positive charge on the β-carbon of the μ-alkylidyne in the transition state for this isomerization.[11,12] Each added alkyl group lowers the barrier for μ-alkylidyne to μ-alkenyl rearrangement by ~7 kcal/mol per β-alkyl substituent.[10] Both the μ-alkylidyne and μ-alkenyl complexes have similar thermodynamic stability in solution with the position of equilibrium for process 2 shifted by β-alkyl substituents.

The relative difference in the "intrinsic" thermodynamic stabilities of the μ-alkylidyne and μ-alkenyl complexes may be accessed by measuring the deprotonation energies of the two isomers in the gas phase.[13] The proton affinity (PA) of a molecule, B, is defined as the negative of the enthalpy change for process 3 in the gas phase. Since only exothermic or near thermoneutral

$$B(g) + H^+(g) \rightarrow BH^+(g) \quad (3)$$

$$PA(B) = -\Delta H^\circ_{rxn} = \Delta H_f^\circ(B) + \Delta H_f^\circ(H^+) - \Delta H_f^\circ(BH^+)$$

ion–molecule reactions proceed with significant rates, the PA of a base can be bracketed by using bases of known PA's, process 4. The relative difference in PA's of two different protonation

$$B_1H^+ + B_2 \rightleftharpoons B_1 + B_2H^+ \quad (4)$$

sites of a neutral may be determined by measuring the difference in the deprotonation energies. This will define the difference in the "intrinsic" thermodynamic stability of the two protonated isomers.

In this contribution the protonation dynamics of $[(C_5H_5)(CO)Fe]_2(\mu\text{-}CO)(\mu\text{-}C{=}CH_2)$ in the gas phase is discussed. The site of protonation and the decomposition processes for protonated $[(C_5H_5)(CO)Fe]_2(\mu\text{-}CO)(\mu\text{-}C{=}CH_2)$ are described.

Experimental Section

The theory, instrumentation, and methodology of ion cyclotron resonance (ICR) spectrometry[14] and Fourier transform mass spectrometry

(3) Nitay, M.; Priester, W.; Rosenblum, M. *J. Am. Chem. Soc.* **1978**, *100*, 3620.
(4) Kao, S. C.; Lu, P. Y.; Pettit, R. *Organometallics* **1982**, *1*, 911.
(5) Dawkins, G. M.; Green, M.; Jeffery, J. C.; Sambale, C.; Stone, F. G. A. *J. Chem. Soc., Dalton Trans.* **1983**, 499.
(6) Casey, C. P.; Fagan, P. J.; Miles, W. H. *J. Am. Chem. Soc.* **1982**, *104*, 1134.
(7) (a) Casey, C. P.; Fagan, P. J. *J. Am. Chem. Soc.* **1982**, *104*, 7360. (b) Casey, C. P.; Fagan, P. J.; Miles, W. H. *J. Am. Chem. Soc.* **1982**, *104*, 1134. (c) Casey, C. P.; Fagan, P. J. *Ibid.* **1982**, *104*, 4950. (d) Casey, C. P.; Fagan, P. J.; Miles, W. H.; Marder, S. R. *J. Mol. Catal.* **1983**, *21*, 173.
(8) Casey, C. P.; Meszaros, M. W.; Fagan, P. J.; Bly, R. K.; Marder, S. R.; Austin, E. A. *J. Am. Chem. Soc.* **1986**, *108*, 4043.
(9) (a) Casey, C. P.; Marder, S. R.; Fagan, P. J. *J. Am. Chem. Soc.* **1983**, *105*, 7197. (b) Casey, C. P.; Meszaros, M. W.; Marder, S. R.; Fagan, P. J. *Ibid.* **1984**, *106*, 3680.
(10) Casey, C. P.; Marder, S. R.; Adams, B. R. *J. Am. Chem. Soc.* **1985**, *107*, 7700 and references cited therein.
(11) Casey, C. P.; Meszaros, M. W.; Fagan, P. J.; Bly, R. K.; Colborn, R. E. *J. Am. Chem. Soc.* **1986**, *108*, 4053.
(12) Casey, C. P.; Meszaros, M. W.; Marder, S. R.; Bly, R. K.; Fagan, P. J. *Organometallics* **1986**, *5*, 1873.
(13) *Gas Phase Ion Chemistry*; Bowers, M. T., Ed.; Academic Press: New York, 1979.
(14) For reviews on ICR see: (a) Beauchamp, J. L. *Annu. Rev. Phys. Chem.* **1971**, *22*, 527. (b) Lehman, T. A.; Bursey, M. M. *Ion Cyclotron Resonance Spectrometry*; Wiley-Interscience: New York, 1976.

(FTMS)[15] have been discussed at length elsewhere. All experiments were performed by using a modified Nicolet FTMS-1000 Fourier transform mass spectrometer equipped with a 5.08 cm cubic trapping cell and 3.0 T superconducting magnet. The spectrometer is controlled by a Nicolet 1280 mini-computer (128 K memory) with data acquisition employing a high-speed digitizer (5.333 MHz, 12 bit) and Fourier transformation facilitated by a 24-bit word array processor.

The main vacuum chamber is evacuated by using a crystal 160 diffusion pump that achieves base pressures in the low 10^{-9} Torr range and the pressure is monitored by a Bayard-Alpert type ionization gauge. The sample inlet system is diffusion pumped (Crystal 63) and modified to include the following: (1) four variable leak sample introduction valves; (2) a General Valve Corporation Series 9 pulsed solenoid valve[16] for temporal variation of neutrals in the main vacuum chamber, and (3) a direct insertion solids probe for introduction of non-volatile samples. Reactive species introduced into the vacuum chamber by the pulsed valve to a pressure of $\sim 10^{-7}$–10^{-6} Torr are pumped away by the high-speed diffusion pump within 500 ms, facilitating more complex experiments.[17]

Chemicals were obtained commercially (except for $[(C_5H_5)(CO)Fe]_2(\mu\text{-}CO)(\mu\text{-}C{=}CH_2)$ and $[(C_5H_5)(CO)Fe]_2(\mu\text{-}CO)(\mu\text{-}CHCH_3)$) in high purity and used as supplied except for multiple freeze–pump–thaw cycles to remove non-condensable gases. $[(C_5H_5)(CO)Fe]_2(\mu\text{-}CO)(\mu\text{-}C{=}CH_2)$ and $[(C_5H_5)(CO)Fe]_2(\mu\text{-}CO)(\mu\text{-}CHCH_3)$ were kindly provided by Professor C. P. Casey.[18] The limited volatility of these diiron complexes required introduction into the vacuum chamber by the direct insertion solids probe. This involved packing a glass capillary tube with 1–2 mg of sample and attaching the tube to the end of the probe. The probe is then inserted into the vacuum chamber and heated to ~100 °C for 1 h to drive off contaminents. This is followed by lowering the probe temperature to 60–80 °C yielding a steady pressure of $1\text{–}2 \times 10^{-8}$ Torr (uncorrected) diiron sample. No impurities were evident in the mass spectra of these diiron complexes after the initial heating.

Argon was used as the collision gas for the collision-induced dissociation (CID)[19] experiments at a total sample pressure of approximately 1×10^{-5} Torr. Details of CID in conjunction with FTMS have been described elsewhere.[20-22] The collision energy of the ions can be varied (typically between 0 and 100 eV) from which plots of CID product ion intensities vs ion kinetic energy can be made. The spread in ion kinetic energy is dependent on the total average kinetic energy and is 65% at 1 eV, 19% at 10 eV, 11% at 30 eV, and 6% at 100 eV.[23]

Results

Proton Affinity of 2. The proton affinity of **2** was determined by the bracketing technique, process 5, employing bases of known proton affinities.[13,24,25] Proton transfer to **2** occurs for all bases

$$BH^+ + \mathbf{2} \rightleftharpoons B + [(C_5H_5)(CO)Fe]_2(\mu\text{-}CO)(\mu\text{-}C{=}CH_2)H^+ \quad (5)$$
$$\mathbf{7}$$

with PA's < 230.1 kcal/mol ($(i\text{-}C_3H_7)_2NH$). Proton transfer from **7** proceeds for bases with PA's > 234.1 kcal/mol ($(n\text{-propyl})_3N$). With $(C_2H_5)_3N$ (PA = 232.3 kcal/mol) an equilibrium is established, process 5, with $K_{eq} \approx 4.5$ (using *uncorrected* ion gauge pressures). From these results, a value of 232.5 ± 2 kcal/mol is assigned for the PA of **2**. The error of 2 kcal/mol is assigned due to the uncertainty in reagent gas pressures.

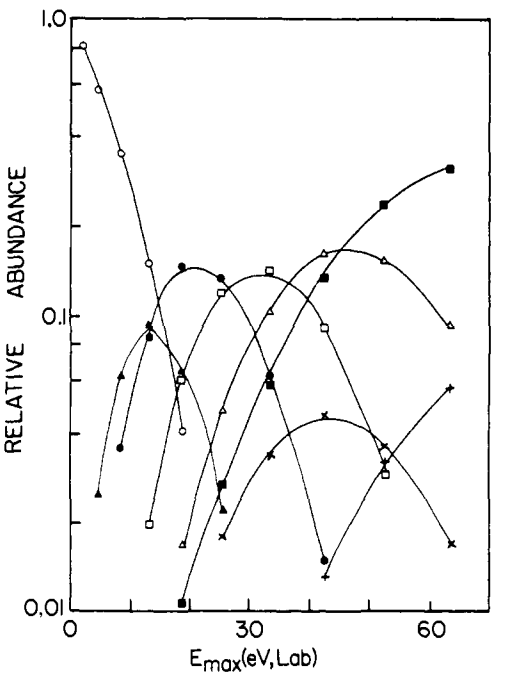

Figure 1. Variation of ion abundances as a function of kinetic energy (laboratory frame) for dissociation of collisionally activated $[(C_5H_5)(CO)Fe]_2(\mu\text{-}CO)(\mu\text{-}C{=}CH_2)H^+$ with argon as the collision gas at a pressure of $\sim 1 \times 10^{-5}$ Torr and with a 30 ms CID interaction time. The relative ion intensities are taken as a fraction of the initial $[(C_5H_5)(CO)Fe]_2(\mu\text{-}CO)(\mu\text{-}C{=}CH_2)H^+$ intensity (no excitation). The sum of the ion abundances totals slightly less than unity at high kinetic energy due to ion losses from the cell. $[(C_5H_5)(CO)Fe]_2(\mu\text{-}CO)(\mu\text{-}C{=}CH_2)H^+$ (○); $(C_5H_5)_2(CO)_2Fe_2C_2H_3^+$ (▲); $(C_5H_5)_2(CO)Fe_2C_2H_3^+$ (●); $[(C_5H_5)Fe]_2C_2H_3^+$ (□); $Fe_2C_{12}H_{11}^+$ (×); $[(C_5H_5)Fe]_2H^+$ (△); $Fe_2C_{10}H_9^+$ (■); $FeC_{10}H_{10}^+$ (+).

Site of Protonation. **2** is readily deuterated by reaction with pyridine-d_5 generating **8**, process 6. **8** reacts with $(CH_3)_2N\text{-}CH_2CH_2N(CH_3)_2$ (PA = 238.8 kcal/mol) to give both protonated

$$C_5D_5ND^+ + \mathbf{2} \rightarrow C_5D_5N + [(C_5H_5)(CO)Fe]_2(\mu\text{-}CO)(\mu\text{-}C{=}CH_2)D^+ \quad (6)$$
$$\mathbf{8}$$

and deuterated $(CH_3)_2NCH_2CH_2N(CH_3)_2$ in a ratio of ~2.6:1. **8** also undergoes thermoneutral proton transfer to **2**, process 7, with the reaction proceeding to completion. These results indicate that **2** is protonated at a site that contains equivalent protons.

$$[(C_5H_5)(CO)Fe]_2(\mu\text{-}CO)(\mu\text{-}C{=}CH_2)D^+ + \mathbf{2} \rightarrow Fe_2C_{15}H_{11}DO_3 + \mathbf{7} \quad (7)$$
$$\mathbf{8}$$

From solution studies, the μ-ethenylidene is protonated on the β-carbon yielding **3**;[3,4] however, both the μ-alkylidyne cation **3** and the corresponding μ-ethenyl cation **6** appear to have similar thermodynamic stability.[9-11] The above labeling results are consistent with protonation at the β-carbon of the μ-ethenylidene group of **2** generating **3**. In this case a statistical proton/deuteron abstraction ratio would be 2:1. The actual ratio of 2.6:1 indicates that proton transfer is favored over deuteron transfer for **8** process 8 this is consistent with a small normal kinetic isotope effect.[26,27] Protonation on the cyclopentadienyl rings cannot be ruled out; however, it seems unlikely. The related complex $[(C_5H_5)(CO)Fe]_2(\mu\text{-}CO)(\mu\text{-}CH_2)$ undergoes protonation on the methylidene[28,29] and $[(C_5H_5)(CO)Fe]_2(\mu\text{-}CO)_2$ undergoes protonation across the

(15) For reviews on FTMS methodology see: (a) Gross, M. L.; Rempel, D. L. *Science (Washington, D.C.)* **1984**, *226*, 26. (b) Wanczek, K. P. *Int. J. Mass Spectrom. Ion Proc.* **1984**, *60*, 11. (c) Marshall, A. G. *Acc. Chem. Res.* **1985**, *18*, 316. (d) Comisarow, M. B. *Anal. Chim. Acta* **1985**, *178*, 1.

(16) General Valve Corporation, 202 Fairfield Road, Fairfield, New Jersey 07006.

(17) A detailed description of pulsed valve introduction of reagent gases in conjunction with FTMS can be found in: Carlin, T. J.; Freiser, B. S. *Anal. Chem.* **1983**, *55*, 571.

(18) Department of Chemistry, University of Wisconsin, Madison, Wisconsin 53715.

(19) Cooks, R. G. *Collision Spectroscopy*; Plenum Press: New York, 1978.

(20) (a) Cody, R. B.; Freiser, B. S. *Int. J. Mass Spectrom. Ion Proc.* **1982**, *41*, 199. (b) Cody, R. B.; Burnier, R. C.; Freiser, B. S. *Anal. Chem.* **1982**, *54*, 96. (c) Burnier, R. C.; Cody, R. B.; Freiser, B. S. *J. Am. Chem. Soc.* **1982**, *104*, 7436.

(21) McIver, R. T., Jr.; Bowers, W. D. *Tandem Mass Spectrometry*; McLafferty, F. W., Ed.; Wiley: New York, 1983; p 287.

(22) Jacobson, D. B.; Freiser, B. S. *J. Am. Chem. Soc.* **1983**, *105*, 736, 7484.

(23) Comisarow, M. B. *J. Chem. Phys.* **1971**, *55*, 187.

(24) Moylan, C. R.; Brauman, J. I. *Annu. Rev. Phys. Chem.* **1983**, *34*, 187.

(25) Proton affinity values are taken from: Lias, S. G.; Liebman, J. F.; Levin, R. D. *J. Phys. Chem. Ref. Data* **1984**, *13*, 695. All values are relative to $PA(NH_3)$ = 204.0 kcal/mol.

(26) Westheimer, F. H. *Chem. Rev.* **1961**, *61*, 265.

(27) More O'Ferrall, R. A. *Proton Transfer Reaction*; Caldin, E., Gold, V., Eds.; Wiley: New York, 1975; Chapter 8.

(28) Casey, C. P.; Fagan, P. J.; Miles, W. H. *J. Am. Chem. Soc.* **1982**, *104*, 1134.

(29) Bursten, B. E.; Cayton, R. H. *Organometallics* **1986**, *5*, 1051 and references cited therein.

Fe–Fe bond yielding $[(C_5H_5)(CO)_2Fe]_2(\mu\text{-}H)^+$.[30]

Decomposition of 7. The variation of ion abundances as a function of kinetic energy for dissociation of collisionally activated (CA) **7** is illustrated in Figure 1. **7** undergoes sequential loss of the three carbonyls as the initial decomposition process. The resulting $[(C_5H_5)Fe]_2C_2H_3^+$ ion, **9**, yields competitive C_2H_2 and H_2 eliminations, processes 8 and 9, with process 8 dominating.

$$([(C_5H_5)Fe]_2C_2H_3^+)^* \text{ (9)} \rightarrow [(C_5H_5)Fe]_2H^+ \text{ (10)} + C_2H_2 \quad (8)$$

$$([(C_5H_5)Fe]_2C_2H_3^+)^* \text{ (9)} \rightarrow Fe_2C_{12}H_{11}^+ + H_2 \quad (9)$$

Ultimately, $Fe_2C_{10}H_9^+$ dominates at high energy. Double resonance indicates that $Fe_2C_{10}H_9^+$ formation from CA of **7** proceeds primarily by the sequential elimination of C_2H_2 and H_2 rather than by direct C_2H_4 elimination. CA of isolated **10** yields *facile* dehydrogenation, reaction 10, along with a small amount of $Fe(C_5H_5)_2^+$ at high energy with no $Fe(C_5H_5)_2H^+$ observed. CA of isolated **11** yields exclusively processes 12 and 13 in low efficiency with process 13 occurring only at high energy.

$$[(C_5H_5)Fe]_2H^+ \text{ (10)} \xrightarrow{CA} Fe_2C_{10}H_9^+ \text{ (11)} + H_2 \quad (10)$$

$$[(C_5H_5)Fe]_2H^+ \text{ (10)} \xrightarrow{CA} Fe(C_5H_5)_2^+ + (FeH) \quad (11)$$

$$Fe_2C_{10}H_9^+ \text{ (11)} \xrightarrow{CA} C_{10}H_9^+ + 2Fe \quad (12)$$

$$Fe_2C_{10}H_9^+ \text{ (11)} \xrightarrow{CA} C_{10}H_8^+ + (Fe_2H) \quad (13)$$

Decomposition of collisionally activated **8** allows the fate of the deuterium label to be monitored. As with **7**, **8** yields initial loss of the three COs forming $[(C_5H_5)Fe]_2C_2H_2D^+$ followed by elimination of C_2H_2, C_2HD, H_2, and HD. Again, elimination of the hydrocarbon fragment dominates over dehydrogenation. The C_2HD:C_2H_2 and the H_2:HD elimination ratios are both ~3:1 for activated $[(C_5H_5)Fe]_2C_2H_2D^+$, reactions 14–17. At high energy

$$([(C_5H_5)Fe]_2C_2H_2D^+)^* \rightarrow [(C_5H_5)Fe]_2H^+ + C_2HD \quad (14)$$

$$([(C_5H_5)Fe]_2C_2H_2D^+)^* \rightarrow [(C_5H_5)Fe]_2D^+ + C_2H_2 \quad (15)$$

$$([(C_5H_5)Fe]_2C_2H_2D^+)^* \rightarrow Fe_2C_{12}H_{10}D^+ + H_2 \quad (16)$$

$$([(C_5H_5)Fe]_2C_2H_2D^+)^* \rightarrow Fe_2C_{12}H_{11}^+ + HD \quad (17)$$

$Fe_2C_{10}H_9^+$ again dominates with no label retained in the ion product. CA of isolated $[(C_5H_5)Fe]_2D^+$ (**12**) yields facile dehydrogenation by eliminating *exclusively* HD, reaction 18, with a small amount of $Fe(C_5H_5)_2^+$ formation at high energy.

$$[(C_5H_5)Fe]_2D^+ \text{ (12)} \xrightarrow{CA} Fe_2C_{10}H_9^+ + HD \quad (18)$$

$$[(C_5H_5)Fe]_2D^+ \text{ (12)} \xrightarrow{CA} Fe(C_5H_5)_2^+ + (FeD) \quad (19)$$

The above results indicate that the deuterium label in **8** is not undergoing scrambling with the cyclopentadienyl ring hydrogens. Furthermore, the high ratio of C_2HD:C_2H_2 elimination provides additional evidence against protonation on the cyclopentadienyl rings. Additional insights into hydrogen migration (hydrogen scrambling) for the above ions may be obtained by monitoring H/D exchange with appropriate exchange agents.[31] No exchange is observed for any of the ions ($[(C_5H_5)(CO)Fe]_2(\mu\text{-}CO)(\mu\text{-}C{=}CH_2)H^+$ through $[(C_5H_5)Fe]_2H^+$) with deuterium.[32] With ethene-d_4, one H/D exchange is observed with the fragment ion $[(C_5H_5)Fe]_2H^+$, process 20, with *no* exchange for the ions $[(C_5H_5)Fe]_2C_2H_3^+$ through $[(C_5H_5)(CO)Fe]_2(\mu\text{-}CO)(\mu\text{-}C{=}CH_2)H^+$ as well as for $[(C_5H_5)Fe]_2D^+$. The exchange, process 20, is the only reaction observed with ethene-d_4 and has a rate

$$[(C_5H_5)Fe]_2H^+ + C_2D_4 \rightarrow [(C_5H_5)Fe]_2D^+ + C_2D_3H \quad (20)$$

constant of $4.0 \pm 2.0 \times 10^{-10}$ cm^3 molecule^{-1} s^{-1}. Comparison with the Langevin collision rate[33] of 9.6×10^{-10} cm^3 molecule^{-1} s^{-1} indicates that the exchange is facile. These results confirm that, upon protonation (deuteration), the proton (deuteron) is not scrambling with the cyclopentadienyl ring hydrogens.

In contrast to ethene, ethyne reacts with **11** yielding both dehydrogenation and condensation, processes 21 and 22, with process 22 dominating. The rate constant for the above reaction is 3.6

$$[(C_5H_5)Fe]_2H^+ + C_2H_2 \text{ (11)} \xrightarrow{10\%} Fe_2C_{12}H_{11}^+ + H_2 \quad (21)$$

$$[(C_5H_5)Fe]_2H^+ + C_2H_2 \text{ (11)} \xrightarrow{90\%} Fe_2C_{12}H_{13}^+ \quad (22)$$

$\pm 2.0 \times 10^{-10}$ cm^3 molecule^{-1} s^{-1} (Langevin[33] collision rate = 8.8×10^{-10} cm^3 molecule^{-1} s^{-1}). The surprising facility of condensation process 22 suggests that the ion-collision complex is long lived and, as a consequence, is stabilized by either infrared radiative stabilization[34,35] or collisional stabilization with argon (~6 ms/collision). The pressure dependence for this stabilization was not investigated. Ethyne undergoes H/D exchange with **12** as well as condensation and dehydrogenation, processes 23–26.

$$[(C_5H_5)Fe]_2D^+ + C_2H_2 \text{ (12)} \rightarrow [(C_5H_5)Fe]_2H^+ + C_2HD \quad (23)$$

$$[(C_5H_5)Fe]_2D^+ + C_2H_2 \text{ (12)} \rightarrow Fe_2C_{12}H_{12}D^+ \quad (24)$$

$$[(C_5H_5)Fe]_2D^+ + C_2H_2 \text{ (12)} \rightarrow Fe_2C_{12}H_{10}D^+ + H_2 \quad (25)$$

$$[(C_5H_5)Fe]_2D^+ + C_2H_2 \text{ (12)} \rightarrow Fe_2C_{12}H_{11}^+ + HD \quad (26)$$

Processes 23 and 24 account for over 90% of the reaction products

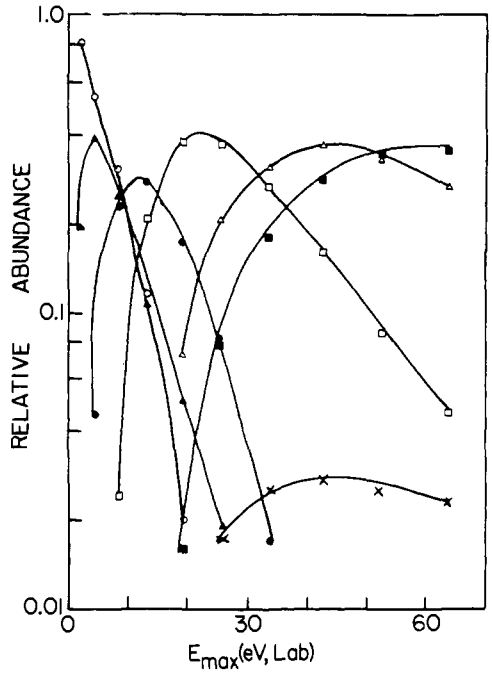

Figure 2. Variation of ion abundances as a function of kinetic energy (laboratory frame) for dissociation of collisionally activated $[(C_5H_5)(CO)Fe]_2(\mu\text{-}CO)(\mu\text{-}C{=}CH_2)^+$ with argon as the collision gas at a pressure of ~1×10^{-5} Torr and with a 30 ms CID interaction time. The relative intensities are taken as a fraction of the initial $[(C_5H_5)(CO)Fe]_2(\mu\text{-}CO)(\mu\text{-}C{=}CH_2)^+$ intensity (no excitation). The sum of the ion abundances totals slightly less than unity at high kinetic energy due to ion losses from the cell. $[(C_5H_5)(CO)Fe]_2(\mu\text{-}CO)(\mu\text{-}C{=}CH_2)^+$ (○); $(C_5H_5)_2(CO)_2Fe_2C_2H_2^+$ (▲); $(C_5H_5)_2(CO)Fe_2C_2H_2^+$ (●); $[(C_5H_5)Fe]_2C_2H_2^+$ (□); $[(C_5H_5)Fe]_2^+$ (×); $FeC_{12}H_{12}^+$ (△); $FeC_{10}H_{10}^+$ (■).

(30) Legzdins, P.; Martin, D. T.; Nurse, C. R.; Wassink, B. *Organometallics* **1983**, *2*, 1238 and references cited therein.

(31) Jacobson, D. B.; Freiser, B. S. *J. Am. Chem. Soc.* **1985**, *107*, 72 and references cited therein.

(32) H/D exchange of organometallic fragment ions with D_2 has been observed. See for example: (a) Byrd, G. D.; Freiser, B. S. *J. Am. Chem. Soc.* **1982**, *104*, 5944. (b) Beauchamp, J. L.; Stevens, A. E.; Corderman, R. R. *Pure Appl. Chem.* **1979**, *51*, 967.

(33) Su, T.; Bowers, M. T. *Gas Phase Ion Chemistry*; Bowers, M. T., Ed.; Academic Press: New York, 1979, Vol 1; Chapter 3.

(34) Woodin, R. L.; Beauchamp, J. L. *Chem. Phys.* **1979**, *41*, 1.

(35) Dunbar, R. C. *Int. J. Mass Spectrom. Ion Phys.* **1983**, *54*, 109.

with an $Fe_2C_{12}H_{12}D^+$:$[(C_5H_5)Fe]_2H^+$ ratio of ~3:1. The $Fe_2C_{12}H_{10}D^+$:$Fe_2C_{12}H_{11}^+$ ratio is 2:1; however, there are significant error bars in this ratio due to the low abundance of the products.

The decomposition of **7** can be compared with the decomposition of $[(C_5H_5)(CO)Fe]_2(\mu\text{-}CO)(\mu\text{-}C{=}CH_2)^+$ (**13**). The variation of ion abundances as a function of kinetic energy for dissociation of collisionally activated **13** is illustrated in Figure 2. As with **7**, **13** yields sequential elimination of the three carbonyls generating $[(C_5H_5)Fe]_2C_2H_2^+$ (**14**). **14** subsequently decomposes to $FeC_{12}H_{12}^+$ and $FeC_{10}H_{10}^+$, processes 27 and 28, with a small amount of $Fe_2C_{10}H_{10}^+$ formed at high energy. $FeC_{10}H_{10}^+$ formation may proceed by direct elimination of FeC_2H_2 or by sequential elimination of an iron atom and C_2H_2. Continuous ejection of $FeC_{12}H_{12}^+$ (mass 212) directly following the excitation of **13** had no effect on $FeC_{10}H_{10}^+$ formation. In addition, CA of $FeC_{12}H_{12}^+$, formed in reaction 27, yields $FeC_5H_5^+$ and Fe^+ as the only fragment ions in low abundance. These results suggest that **14** undergoes competitive elimination of Fe and FeC_2H_2. Furthermore, the direct elimination of FeC_2H_2, process 28, becomes more favorable as the collision energy is increased.

$$[(C_5H_5)Fe]_2C_2H_2^{+*} \;(\mathbf{14}) \longrightarrow \begin{cases} FeC_{12}H_{12}^+ + Fe & (27) \\ FeC_{10}H_{10}^+ + (FeC_2H_2) & (28) \\ Fe_2C_{10}H_{10}^+ + C_2H_2 & (29) \end{cases}$$

Reactivity of 7 with Carbon Electrophiles. The reactivity of **7** with carbon electrophiles (aldehydes and ketones) was investigated. No reaction was observed between **7** and aldehydes (acetaldehyde, *p*-tolualdehyde, cinnamaldehyde) or acetone.

Hydride Abstraction from $[(C_5H_5)(CO)Fe]_2(\mu\text{-}CO)(\mu\text{-}CHCH_3)$. Hydride abstraction from $[(C_5H_5)(CO)Fe]_2(\mu\text{-}CO)(\mu\text{-}CHCH_3)$ (**15**) by a number of radical cations was attempted,[10] process 30. In every case, either proton transfer or charge transfer was observed. For example, $c\text{-}C_7H_7^+$ yields exclusively charge transfer, process 31, implying IP(**15**) < 6.24 eV.[36] For comparison, the IP of $[(C_5H_5)(CO)Fe]_2(\mu\text{-}CO)_2$ is 6.95 eV.[37] Hence, replacement of a μ-CO by a μ-alkylidene lowers the IP of the complex by at least 0.7 eV.

$$A^+ + \mathbf{15} \rightarrow AH + [(C_5H_5)(CO)_2Fe]_2(\mu\text{-}CO)(C_2H_3)^+ \quad (30)$$

$$c\text{-}C_7H_7^+ + \mathbf{15} \rightarrow c\text{-}C_7H_7 + [(C_5H_5)(CO)Fe]_2(\mu\text{-}CO)(\mu\text{-}CHCH_3)^+ \quad (31)$$

Discussion

Protonation and Reactivity. As in solution **2** appears to undergo protonation at the β-carbon of the μ-ethenylidene generating **3** in the gas phase. The site of protonation clearly contains equivalent hydrogens as evidenced by the deprotonation/dedeuteration results for **8**. Protonation on the cyclopentadienyl rings would yield a complex containing equivalent hydrogens and, therefore, cannot be unequivocally dismissed. This seems unlikely, however, since both $[(C_5H_5)(CO)Fe]_2(\mu\text{-}CO)(\mu\text{-}CH_2)$[28,29] and $[(C_5H_5)(CO)Fe]_2(\mu\text{-}CO)_2$[30] do not protonate on the cyclopentadienyl rings in solution. The CA results for **8** are also consistent with protonation at the β-carbon of the μ-ethenylidene of **2**, vide infra.

Assuming that protonation of **2** generates **3** implies that **3** is thermally more stable than bridging ethenyl species **6**. In solution, both bridging alkylidyne- and bridging alkenyl-diiron ions have similar thermodynamic stability.[10] In the gas phase the "intrinsic" thermodynamic stability is probed, whereas in solution both the "intrinsic" stability as well as solvation effects must be considered.[13,24,25] Hence these gas-phase results suggest that μ-alkenyl **6** must be stabilized more by solvation than corresponding μ-ethylidyne **3**. Interestingly, μ-alkylidyne complexes are deprotonated much more rapidly than the corresponding μ-alkenyl species in solution.[9a,10] Although there are several possible explanations for this behavior, it may simply reflect the difference in solvation energy of the two isomers where the increased solvation energy of the μ-alkenyl renders it less accessible to proton transfer.

The difference in the intrinsic stability of **3** and **6** may be accessed in the gas phase by measuring the difference in their deprotonation energies. This requires that **3** and **6** do not interconvert in the gas phase. This seems reasonable since the barrier for their interconversion ($\Delta G^{\ddagger}$) is greater than 31 kcal/mol in solution.[9a] It is very likely that a similar barrier would exist for this interconversion in the gas phase as well. Hence, it should be possible to generate **3** and **6** and probe their deprotonation energies. Attempts to synthesize μ-ethenyl **6** by hydride abstraction of **15** by a number of cations were unsuccessful.[10]

The proton affinity of **2** was bracketed as 232.5 ± 2 kcal/mol. This high value for the PA of **2** is consistent with the high thermal stability of **3** in solution. Casey has suggested that extensive electron donation from the two iron centers is responsible for the stability of the μ-alkylidyne species.[7] Such a donation would, in turn, contribute to the high PA of the corresponding μ-ethenylidene **2** as observed. For comparison, PA($Fe(C_5H_5)_2$) = 210 kcal/mol and PA($(C_5H_5)Fe(CO)_2CH_3$) = 190.6 kcal/mol.[25]

The electronic structures of **2**, **4**, and **5** have been investigated via nonempirical Fenske–Hall molecular orbital calculations.[38] These results reveal that the framework orbitals for $[(C_5H_5)(CO)Fe]_2(\mu\text{-}CO)(\mu\text{-}R)$ are of π-symmetry and oriented perpendicular to the Fe–(μ-C)–Fe plane. The bridging $-C{=}CH_2$ (ethenylidene) contains a C–C π bond that is also oriented perpendicular to the Fe–(μ-C)–Fe plane; however, it interacts only slightly with the dimer framework. The bridging $-CH^+$ (methylidyne) has an empty set of doubly degenerate π orbitals (π_x and π_y). The π_y orbital is oriented perpendicular to the Fe–(μ-C)–Fe plane and interacts significantly with a framework orbital. The bonding of a μ-C^+–CH_3 (ethylidyne) to the dimer framework should be very similar to that for μ-CH^+. Hence, upon protonation of the μ-$C{=}CH_2$ ligand forming μ-C^+–CH_3 there is a significant change in the electronic structure allowing for flow of electron density from the diiron framework into an empty π_y orbital of C^+–CH_3 which, apparently, contributes to the high PA of **2**.

In solution, (μ-alkylidyne)diiron **3** reacts with aldehydes (acetaldehyde, *p*-tolualdehyde, cinnamaldehyde) and acetone producing new cationic vinylcarbyne complexes,[39] reaction 32. The postulated mechanism for this reaction is shown below and involves initial proton transfer to the carbonyl electrophile.[39] μ-Alkylidene complex **2** acts as a nucleophile attacking the protonated carbonyl yielding **17** followed by water elimination producing vinylcarbyne complex **16**. The key step in this mechanism is the carbon–carbon

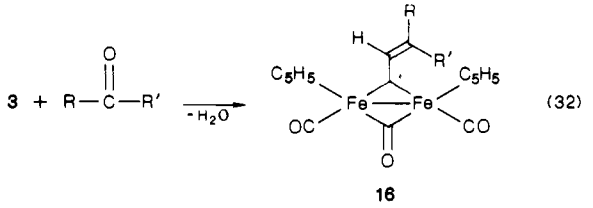

(32)

16

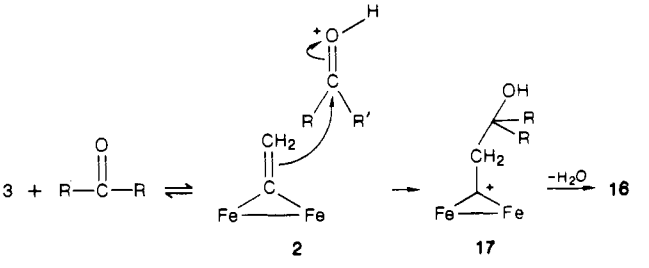

2 **17**

(36) Supplemental thermochemical information taken from: Rosenstock, H. M.; Draxl, K.; Steiner, B. W.; Herron, J. T. *J. Phys. Chem. Ref. Data Suppl. 1* **1979**, *6*.

(37) Granozzi, G.; Tondello, E.; Benard, M.; Fragala, I. *J. Organomet. Chem.* **1980**, *194*, 83.

(38) Bursten, B. E.; Cayton, R. H. *J. Am. Chem. Soc.* **1986**, *108*, 8241; **1987**, *109*, 6053.

(39) Casey, C. P.; Konings, M. S.; Palermo, R. E.; Colborn, R. E. *J. Am. Chem. Soc.* **1985**, *107*, 5296.

bond formation by nucleophilic attack of the protonated carbonyl.

In the gas phase μ-ethylidyne **3** is inert toward the above carbonyl species. The first step in the above mechanism involves proton transfer to the organic carbonyl. In the gas phase *endothermic* proton transfer in an ion–molecule collision complex can occur,[40,41] e.g., process 33, and this transfer is driven by the ion-induced dipole attractive energy that is typically 20 kcal/mol.[42]

$$B + AH^+ \rightleftharpoons (AH^+)(B)^* \rightleftharpoons (A)(BH^+)^* \qquad (33)$$

The proton affinities (PAs) of the above carbonyl species ranged from 186.6 kcal/mol for acetaldehyde to 203.7 kcal/mol for *p*-tolualdehyde.[25] Since the PA of **2** is 232.5 ± 2 kcal/mol, then there will be insufficient energy in the ion–molecule collision complex to *drive* the endothermic proton transfer required for reaction 32. Hence, the inert behavior of these carbonyls with **3** is *consistent* with the above mechanism for reaction 32 in solution.

Decomposition of 7. Decomposition of collisionally activated organometallic ions yields a wealth of information concerning structure, dissociation pathways, and dynamics of rearrangements.[43] Here, dissociation results from inelastic collisions of a polyatomic ion, possessing a desired kinetic energy (typically <150 eV), with a neutral target molecule. Such a method of exciting polyatomic ions is coined "collisional activation" (CA), and dissociation resulting from this excitation is referred to as "collision-induced dissociation" (CID). At the translational energies employed in this study (<150 eV) internal energy transfer upon inelastic collisions involves direct vibrational excitation.[44,45] Activated polyatomic ions can survive many vibrations prior to dissociating, hence, the CID process proceeds through a two-step sequence involving excitation followed by fragmentation.[45,46] Dissociation of collisionally activated ions under the conditions of the FTMS experiment involves incremental increases in the internal energy of the ion by multiple collisions with the collision gas atoms (molecules)[20c,22,47] as depicted in process 34. As a

$$A^+ \xrightarrow{N} (A^+)^* \xrightarrow{N} (A^+)^{**} \xrightarrow{N} \qquad (34)$$

consequence low-energy rearrangements followed by elimination of the thermally most favorable neutrals are facilitated. These concepts will be useful in interpreting the CID processes observed for these diiron complex ions.

Facile elimination of the three carbonyls from CA of **7** implies $D°[(C_5H_5)_2Fe_2(CO)_{x-1}(\mu\text{-}C\text{-}CH_3)^+\text{-}CO] < D°[(C_5H_5)_2Fe_2(CO)_x^+\text{-}(\mu\text{-}C\text{-}CH_3)]$ for $x = 1\text{-}3$. This is expected since the elimination of carbonyls from activated transition-metal cluster carbonyl ions is, in general, a facile process.[48,49] In addition, the binding energy of the μ-ethylidyne should be much greater than that for the carbonyls, vide supra.[38] An additional fragmentation process to consider is the direct cleavage of diiron **7** such as reactions 35 and 36. The photochemistry of a number of dinuclear

$$7 \xrightarrow{CA} (C_5H_5)Fe(CO)(\mu\text{-}C{=}CH_2)^+ + (C_5H_5)Fe(CO)_2H \qquad (35)$$

$$7 \xrightarrow{CA} (C_5H_5)Fe(CO)(\mu\text{-}C\text{-}CH_3)^+ + (C_5H_5)Fe(CO)_2 \qquad (36)$$

metal–metal bonded complexes including $[(C_5H_5)(CO)_2Fe]_2$ and $[(C_5H_5)(CO)_2Ru]_2$ yields both mononuclear radicals (metal–metal bond cleavage)[50-53] as well as CO elimination (no metal–metal bond cleavage).[52,54-56] In this case absorption of a photon involves electronic excitation and not direct vibrational excitation. CID of both $[(C_5H_5)(CO)_2Fe]_2^+$ and $[(C_5H_5)(CO)_2Fe]_2H^+$ in the gas phase is similar to that for **7** and it is dominated by decarbonylation with no evidence for initial metal–metal bond cleavage.[57]

Elimination of C_2H_2 from the activated $[(C_5H_5)Fe]_2C_2H_3^+$ fragment, **9**, (process 8) probably proceeds by initial rearrangement of a μ-ethylidyne to a μ-ethenyl (e.g., process 2) followed by β-hydrogen elimination with subsequent ethyne loss, process 37. The rearrangement of **17** to **18** has relevance to the surface-mediated formation of μ-ethylidyne from chemisorbed ethene.[58] The reversible insertion of coordinated alkynes into metal–hydrogen bonds is well established[59,60] and it is the crucial step in the hydrogenation of alkynes to alkenes.[61] The above mechanism for C_2H_2 elimination (process 37) requires that the barrier for the 1,2 hydrogen shift (i.e., conversion of **17** to **18**) be less than the energy necessary for direct elimination of C_5H_5 or CCH_3 from **17**. This seems reasonable since the barrier for this rearrangement for **3** in solution is probably less than 40 kcal/mol[10] and the binding energy of C_5H_5 and CCH_3 should be considerably greater than this barrier.

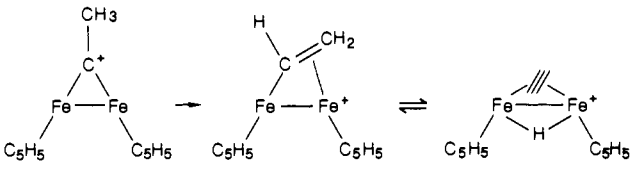

(37)

The above mechanism (process 37) for C_2H_2 elimination is supported by labeling studies as well as H/D exchange. For example, the interconversion between **18** and **19** can be explored by monitoring H/D exchange of **12** with ethyne. Ethyne undergoes H/D exchange with **12**, process 23, as well as competitive condensation, process 24. Since the condensation process is rapid it will compete with alternative reaction channels (i.e., the exchange process). Hence, observation of significant H/D exchange, process 23, implies that this exchange is facile. There are two reasonable mechanisms to consider for this exchange. The first simply involves the interconversion of **19** and **18** as shown in process 37. The second involves reversible insertion into a C–H bond of ethyne, process 38. Although the dynamics of these two processes (i.e., interconversion of **19** and **18** or **19** and **20**) are quite speculative we believe that the conversion of **19** to **20** is thermally less favorable with intermediate **20** ca. 30 kcal/mol less stable

(40) (a) Freiser, B. S.; Woodin, R. L.; Beauchamp, J. L. *J. Am. Chem. Soc.* **1975**, *97*, 6893. (b) Hunt, D. F.; Sethi, S. K. *Ibid.* **1980**, *102*, 6953 and references cited therein.
(41) (a) Grabonski, J. J.; DePuy, C. H.; Bierbaum, V. M. *J. Am. Chem. Soc.* **1983**, *105*, 2565. (b) Squires, R. R.; Bierbaum, V. M.; Grabowski, J. J.; DePuy, C. H. *Ibid.* **1983**, *105*, 5185 and references cited therein.
(42) Magnoli, D. E.; Murdock, J. R. *J. Am. Chem. Soc.* **1981**, *103*, 7465.
(43) Jacobson, D. B.; Fresier, B. S. *J. Am. Chem. Soc.* **1983**, *105*, 5197.
(44) Yost, R. A.; Enke, C. G.; McGilvery, D. C.; Smith, D.; Morrison, J. D. *Int. J. Mass Spectrom. Ion Phys.* **1976**, *30*, 127.
(45) Douglas, D. J. *J. Phys. Chem.* **1982**, *86*, 185.
(46) McLafferty, F. W.; Todd, P. J.; McGilvery, D. C.; Baldwin, M. A.; Bockhoff, M. B.; Wendel, G. J.; Wixom, M. R.; Niemi, J. E. *Advances in Mass Spectrometry*; Quayle, B. A., Ed.; Heydon: London, 1980.
(47) Kenttamaa, H. I.; Cooks, R. G. *Int. J. Mass Spectrom. Ion Proc.* **1985**, *64*, 79.
(48) Jacobson, D. B.; Freiser, B. S. *J. Am. Chem. Soc.* **1984**, *106*, 4623.
(49) Hettich, R. L.; Jackson, T. C.; Stanko, E. M.; Freiser, B. S. *J. Am. Chem. Soc.* **1986**, *108*, 5086.
(50) (a) Abrahamson, H. B.; Wrighton, M. S. *Inorg. Chem.* **1978**, *17*, 1003. (b) Ginnotti, C.; Merle, G. J. *Organomet. Chem.* **1976**, *105*, 97.
(51) Abrahamson, H. B.; Palazzoto, M. C.; Reichel, C. L.; Wrighton, M. S. *J. Am. Chem. Soc.* **1979**, *101*, 4123.
(52) Caspar, J. V. *J. Am. Chem. Soc.* **1980**, *102*, 7794.
(53) (a) Moore, B. D.; Poliakoff, M.; Turner, J. J. *J. Am. Chem. Soc.* **1986**, *108*, 1819. (b) Dixon, A. J.; Healy, M. A.; Poliakoff, M.; Turner, J. T. *J. Chem. Soc., Chem. Commun.* **1986**, 994.
(54) Hooker, R. H.; Rest, A. J. *J. Chem. Soc., Chem. Commun.* **1983**, 1022.
(55) Hepp, A. F.; Blaha, J. P.; Lewis, C.; Wrighton, M. S. *Organometallics* **1984**, *3*, 174.
(56) Tyler, D. R.; Schmidt, M. A.; Gray, H. B. *J. Am. Chem. Soc.* **1983**, *105*, 6018.
(57) Jacobson, D. B. Unpublished results.
(58) (a) Kesmodel, L. L.; Dubois, L. H.; Somorjia, G. A. *Chem. Phys. Lett.* **1978**, *92*, 240 and references cited therein. (b) Davis, S. M.; Zaera, F.; Gordon, B. E.; Somorjia, G. A. *J. Catal.* **1985**, *92*, 240 and references cited therein.
(59) Werner, H.; Esteruelas, M. A.; Otto, H. *Organometallics* **1986**, *5*, 2295.
(60) (a) Amandrut, J.; Leblanc, J.-C.; Moise, C.; Sala-Pala, J. J. *J. Organomet. Chem.* **1985**, *295*, 167. (b) Herberich, G. E.; Barlage, W. *Organometallics* **1987**, *6*, 1924. (c) Bianchini, C.; Innocenti, P.; Masi, D.; Meli, A.; Sabat, M. *Ibid.* **1986**, *5*, 72.
(61) (a) Stolzenberg, M. A.; Muetterties, E. L. *Organometallics* **1985**, *4*, 1739. (b) Sanchez-Delgado, R. A.; Andriolla, A.; Gonzalez, E.; Valencia, N.; Leon, V.; Espidel, J. J. *J. Chem. Soc., Dalton Trans.* **1985**, 1859.

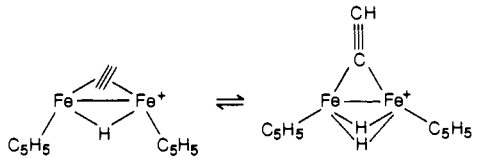

19 20

than **19**.[62] In contrast, **18** and **19** are estimated to have similar thermodynamic stability with **19** being slightly more stable.[62] Hence, the H/D exchange, process 23, probably proceeds by reversible insertion of coordinated ethyne into the diiron–hydrogen bond as depicted in the mechanism for process 37 and this is driven by the diiron–ethyne binding energy.

Facile H/D exchange of **10** with ethene-d_4, process 20, probably proceeds by reversible insertion of coordinated ethene into a diiron hydride as shown in process 39. The facility of this exchange requires a low barrier for this process.[64] Only one exchange is

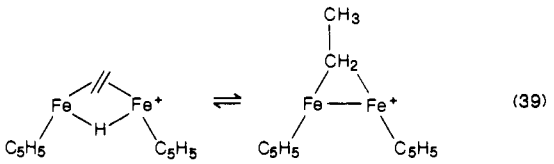

observed for **10**, indicating that the exchangeable hydrogen is not undergoing scrambling with the ring hydrogens. Absence of exchange of **12** with ethene-d_4 confirms that the exchangeable hydrogen does not involve the ring hydrogens and that this hydrogen originates from the initial site of protonation. Furthermore, the deuteron of **8** is scrambled with the hydrogens of the μ-ethenylidene upon fragmentation by CA, processes 14 and 15.

Absence of scrambling of the ring hydrogens in **10** with the unique, exchangeable hydrogen contrasts that observed for the related $FeC_5H_6^+$ system where the following equilibrium is facile with all the hydrogens scrambled by exo-hydrogen [1,5] sigma-

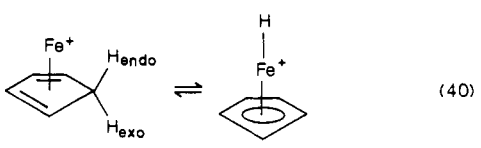

21 22

tropic shifts in **21**.[31,65] Such a process is thermally allowed in the ground state[66] and has a barrier of 23.6 kcal/mol for isolated cyclopentadiene.[67] The barrier for exo-hydrogen [1,5] sigmatropic shifts in **21** appears to be much less than that for isolated cyclopentadiene.[31] Exo-hydrogen [1,5] sigmatropic shifts have been invoked to explain hydrogen scrambling in the following system.[68] Absence of scrambling of the cyclopentadienyl ring hydrogens in

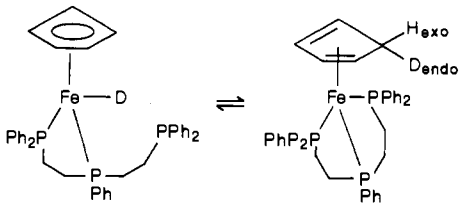

10 suggests a barrier for H/D scrambling in excess of the binding energy of ethene to **10**. This may be due to either a larger barrier for formation of **24** from **23** or to a large barrier for exo-hydrogen [1,5] sigmatropic shifts for the cyclopentadiene ligand in **24**. The former is a more likely feature.

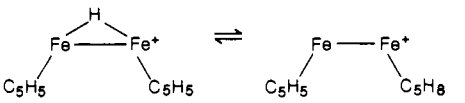

23 24

Absence of H/D exchange for $[(C_5H_5)Fe]_2C_2H_3^+$ with ethene-d_4 is particularly significant in that it provides additional evidence for protonation on the β-carbon of the μ-ethenylidene in **2**. It has already been established that species **18** and **19** are rapidly interconverting. As a consequence H/D exchange would be expected upon interaction of ethene-d_4 with either **18** or **19** where the exchange would proceed by a similar mechanism to that for interaction of ethene-d_4 with **10**. It is possible that the addition of ethyne to **10** (i.e., **19**) changes the dynamics for the exchange process with ethene-d_4 resulting in a large barrier for the reversible insertion of coordinated ethene into the metal hydrogen bond. A more likely explanation is that $[(C_5H_5)Fe]_2(C_2H_3)^+$ contains a μ-ethylidyne unit, **17**, and that the barrier for conversion of **17** to **18** by a 1,2-hydrogen shift is greater than the binding energy of ethene to **17**. We estimate that the binding energy of ethene to **17** is in the range of 30–40 kcal/mol, hence, the barrier for the 1,2-hydrogen shift for converting **17** to **18** must exceed this value. For comparison, the barrier for this rearrangement of **3** in solution is greater than 31 kcal/mol and is probably less than 40 kcal/mol.[10]

The partitioning of the deuterium label in the decomposition of **8** can yield additional insights into the mechanism and dynamics of the decomposition processes. In particular, the C_2HD/C_2H_2 and H_2/HD elimination ratios for activated $[(C_5H_5)Fe]_2C_2H_2D^+$ are informative, reactions 14–17. This ion initially consists of structure **17** which rearranges to **18** by a 1,2-hydrogen (deuterium) shift. Facile interconversion of **18** and **19** results in scrambling of the deuterium label followed by competitive elimination of ethyne and dihydrogen. Statistical scrambling of the label with the two hydrogen atoms would yield a $C_2HD:C_2H_2$ elimination ratio of 2:1. The actual ratio is 3:1, indicating preferential elimination of the label in ethyne. Dehydrogenation probably proceeds by elimination of one ring hydrogen atom, vide infra, which would yield an H_2:HD ratio of 2:1 for statistical scrambling. The actual ratio of 3:1 (H_2:HD) is consistent with the ratio for label in ethyne loss. These results can be interpreted by invoking a kinetic isotope effect that favors retention of the label on the hydrocarbon fragment.[68]

The decomposition of collisionally activated $[(C_5H_5)Fe]_2H^+$ (**10**) can be compared to that for $Fe_2(C_5H_5)_2^+$ where facile elimination of an iron atom is the only process observed,[69] reaction

(62) Using $D°\{[(C_5H_5)Fe]_2H^+–C_2H_2\}$ = 50 kcal/mol, $D°\{[(C_5H_5)Fe]_2^+–H\}$ = 70 kcal/mol, $D°\{[(C_5H_5)Fe]_2^+–CHCH_2\}$ = 100 kcal/mol and auxiliary thermochemical information from ref 36 and 63 the following rearrangement

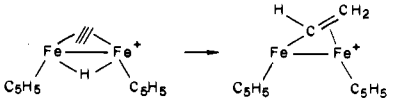

is calculated to ~16 16 kcal/mol exothermic. Using the above information as well as $D°\{[(C_5H_5)Fe]_2(H)_2^+–CCH\}$ = 70 kcal/mol and $D°\{[(C_5H_5)Fe]_2H^+–H\}$ = 60 kcal/mol the following rearrangement

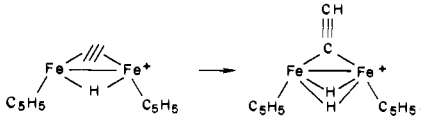

is calculated to be ~32 kcal/mol endothermic.

(63) Thermochemical information for hydrocarbon radicals from: McMillen, D. F.; Golden, D. M. *Annu. Rev. Phys. Chem.* **1982**, *33*, 493.

(64) Kinetic studies have revealed that the reversible insertion of a coordinated alkene into a metal–hydrogen bond is, in general, facile. See, for example: (a) Collman, J. P.; Hegedus, L. S. *Principles and Applications of Organotransition Metal Chemistry*; University Science Books: Mil Valley, CA 1980. (b) Doherty, N. M.; Bercaw, J. E. *J. Am. Chem. Soc.* **1985**, *107*, 2670, and references cited therein.

(65) Jacobson, D. B.; Freiser, B. S. *J. Am. Chem. Soc.* **1983**, *105*, 7492.

(66) Sprangler, C. W. *Chem. Rev.* **1976**, *76*, 187.

(67) (a) Roth, W. *Tetrahedron Lett.* **1964**, 1009. (b) Berson, J. A.; Aspelin, G. G. *Tetrahedron* **1964**, *20*, 2697.

(68) The lowest energy configuration for the reaction intermediate is deuterium bonded to carbon and not the metal. The effect of the zero-point-energy differences for isotopically distinct structure **19** is responsible for this behavior.

41. By analogy, $[(C_5H_5)Fe]_2H^+$ may decompose by either process 11 (FeH elimination) or 42 with process 42 roughly 26 kcal/mol

$$Fe(C_5H_5)_2^+ \xrightarrow{CA} Fe(C_5H_5)_2^+ + Fe \qquad (41)$$

$$[(C_5H_5)_2Fe]_2H^+ \xrightarrow{CA} Fe(C_5H_5)_2H^+ + Fe \qquad (42)$$

more favorable than process 11.[70] The dominant decomposition process for activated $[(C_5H_5)Fe]_2H^+$ is neither process 11 nor 42 but, rather, facile dehydrogenation. This dehydrogenation, process 10, may proceed by the abstraction of one ring hydrogen yielding a bridging η^1:η^5-cyclopentadienyl complex, **25**, or by the direct coupling of the two cyclopentadienyl ligands to give an η^5:η^5-fulvalene complex, **26**. Complexes containing a bridging

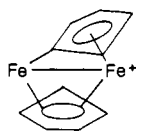

25

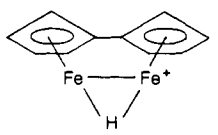

26

η^1:η^5-cyclopentadienyl group have been characterized,[71-73] and the coupling of cyclopentadienyl ligands in transition-metal complexes yielding η^5:η^5-fulvalene–dimetal complexes is a common process.[74] If dehydrogenation of $[(C_5H_5)Fe]_2H^+$ proceeds by direct formation of **26**, then the hydrogen atoms eliminated would originate from the cyclopentadienyl ligands. The exclusive elimination of HD upon CA of $[(C_5H_5)Fe]_2D^+$, however, suggests that this dehydrogenation proceeds by formation of a bridging η^1:η^5-cyclopentadienyl species, **25**. The bimetallic dimer, $CoFe^+$, dehydrogenates monomeric cyclopentadiene, process 43, presumably generating a bridging η^1:η^5-cyclopentadienyl species.[75] If dehydrogenation of $[(C_5H_5)Fe]_2H^+$ is generating **26** directly then

$$CoFe^+ + c\text{-}C_5H_6 \rightarrow CoFeC_5H_4^+ + H_2 \qquad (43)$$

dehydrogenation upon CA of $Fe_2(C_5H_5)_2^+$ would also be expected. That CA of $Fe_2(C_5H_5)_2^+$ yields no dehydrogenation[69] provides additional support for the formation of **25** from dehydrogenation of activated $[(C_5H_5)Fe]_2H^+$.

Collision activation of the above dehydrogenation product, $Fe_2C_{10}H_9^+$, yields exclusively $C_{10}H_9^+$ and $C_{10}H_8^+$, processes 12 and 13. This suggests that the two cyclic C_5 ligands have coupled. This coupling presumably forms **26** and must take place after dehydrogenation, vide supra.

Decomposition of 13. The decomposition of collisionally activated **7** and **13** shows dramatic differences as seen in Figures 1 and 2. Both ions yield facile and sequential elimination of the three carbonyls yielding **9** and **14**. Whereas **9** yields competitive C_2H_2 and H_2 eliminations, processes 8 and 9, **14** undergoes competitive elimination of an iron atom and FeC_2H_2, processes 27 and 28. **14** presumably consists of bridging ethenylidene **27**, where the cyclopentadienyl rings may be bridging the Fe–Fe unit

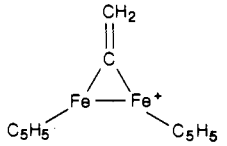

27

as in Pd_2,[76,77] PdPt,[78] and Pt_2[79] complexes. The energy dependency for the decomposition of **13** (Figure 2) suggests the existence of a kinetic barrier to decomposition of **14** (mass 268) which is not present for **9** (mass 269) in Figure 1.

Elimination of either an iron atom or an FeC_2H_2 unit for **14** is clearly a difficult process. Observation that process 28 becomes more competitive with process 27 as the collision energy increases combined with the absence of $FeC_{10}H_{10}^+$ formation upon CA of $FeC_{12}H_{12}^+$ suggests that process 27 may involve substantial rearrangement of the hydrocarbon network whereas process 28 may involve more direct processes. The absence of C_2H_2 elimination combined with the overall inefficient fragmentation of $FeC_{12}H_{12}^+$ upon CA suggests that the C_2H_2 unit has been incorporated into the cyclopentadienyl rings. A structure for $FeC_{12}H_{12}^+$ that is consistent with the above results in ferrocene-1,1′-(1,2-ethanediyl), **28**, which has previously been observed.[80,81] Such a rearrangement

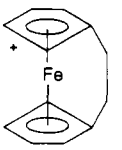

28

may involve prior isomerization of the μ-ethenylidene in **27** to a coordinated ethyne by a 1,2-hydrogen atom shift followed by a coupling of the cyclopentadienyl rings by ethyne. The reverse of the above isomerization (i.e., rearrangement of terminal alkynes to alkenylidenes) is well established for transition-metal catalysts.[82-84]

Formation of $FeC_{10}H_{10}^+$ dominates at high energy and is formed by the direct elimination of FeC_2H_2 from **14**. This energy dependence implies elimination of FeC_2H_2 as iron–ethenylidene. Complete retention of the charge by the product, $FeC_{10}H_{10}$, implies $IP(FeC_2H_2) > IP(Fe(C_5H_5)_2) = 6.88$ eV.[70]

The above results clearly show the influence that an additional hydrogen atom exerts on the processes accessible for decomposition of these diiron species.

Conclusions

The proton affinity (PA) of **2** in the gas phase is quite high (PA = 232.5 ± 2 kcal/mol) and the site of protonation is the β-carbon of the μ-ethenylidene group yielding **3** in accord with the solution chemistry of **2**. The high PA of **2** forming **3** is attributed to the strong interaction of the perpendicularly oriented π-orbital of the Fe–(μ-C)–Fe framework with an empty π_y orbital of the μ-C^+–CH_3 group.[38] The synthesis of the isomeric μ-alkenyl complex, **6**, was pursued in an effort to distinguish the "intrinsic" difference in the thermal stability of **3** and **6**. Efforts to generate isomeric species **6** were unsuccessful; however, it is clearly thermally less stable than **3**. Since **3** and **6** have similar thermodynamic stability in solution then **6** must be more strongly solvated than **3**.

The reactivity and decomposition processes of **3** were studied in detail. **3** is completely inert in the gas phase, even with carbonyl

(69) Jacobson, D. B.; Freiser, B. S. *Organometallics* **1985**, *4*, 1048.
(70) Thermochemical data from ref 25 and 36. $IP(FeCp_2) = 6.88$ eV from: Green, J. C. *Struct. Bonding (Berlin)* **1981**, *43*, 37. $\Delta H_f°(FeH) = 122 \pm 3$ kcal/mol from: Sallams, L.; Lane, K. R.; Squires, R. R.; Freiser, B. S. *J. Am. Chem. Soc.* **1985**, *107*, 4379.
(71) Pez, G. P. *J. Am. Chem. Soc.* **1976**, *98*, 8072.
(72) Hoxmeier, R.; Deubser, B.; Kaesz, H. D. *J. Am. Chem. Soc.* **1971**, *93*, 536.
(73) (a) Guggenberger, L. J. *Inorg. Chem.* **1973**, *12*, 294. (b) Forder, R. A.; Green, M. L. H.; Mckenzie, R. E.; Poland, J. S.; Prout, K. *J. Chem. Soc., Chem. Commun.* **1973**, 426. (c) Baker, E. C.; Raymond, K. N.; Marks, T. J.; Watcher, W. A. *J. Am. Chem. Soc.* **1974**, *96*, 7586.
(74) McKinney, R. J. *J. Chem. Soc., Chem. Commun.* **1980**, 603.
(75) Jacobson, D. B.; Freiser, B. S. *J. Am. Chem. Soc.* **1985**, *107*, 1581.
(76) (a) Werner, H.; Tune, D.; Parker, G.; Jrygerm, C.; Brauer, D. J. *Angew. Chem., Int. Ed. Engl.* **1975**, *14*, 185. (b) Kuhn, A.; Werner, H. *J. Organomet. Chem.* **1979**, *179*, 421.
(77) (a) Werner, H.; Kraus, H. J. *J. Chem. Soc., Chem. Commun.* **1979**, 814. (b) Werner, H.; Kraus, H. J. *Angew. Chem., Int. Ed. Engl.* **1979**, *18*, 948.
(78) (a) Werner, H.; Kraus, H. J. *Chem. Ber.* **1980**, *113*, 1072. (b) Werner, H.; Kuhn, A. *Z. Naturforsch., Teil B* **1978**, *33*, 1360.
(79) (a) Werner, H.; Kuhn, A.; Burschka, C. *Chem. Ber.* **1980**, *113*, 2291. (b) Werner, H.; Kuhn, A. *Angew. Chem., Int. Ed. Engl.* **1977**, *16*, 412.
(80) These structures are more commonly referred to as ferrocenophanes.
(81) (a) Vogtle, F.; Neuman, P. *Tetrahedron* **1970**, *26*, 5847. (b) Watts, W. E. *Organomet. Chem. Rev.* **1967**, *2*, 231. (c) Mueller-Westerhoff, U. T. *Angew. Chem., Int. Ed. Engl.* **1986**, *25*, 702 and references cited therein.
(82) Bruce, M. I.; Swincer, A. G. *Adv. Organomet. Chem.* **1983**, *22*, 59.
(83) (a) Landon, S. J.; Shulmen, P. M.; Geoffrey, G. L. *J. Am. Chem. Soc.* **1985**, *107*, 6739. (b) Birdwhistell, K. R.; Burgmayer, S. J. N.; Templeton, J. L. *Ibid.* **1983**, *105*, 7789.
(84) Bates, D. J.; Rosenblum, M.; Samuels, S. B. *J. Organomet. Chem.* **1981**, *209*, C55.

electrophiles. This inert behavior is consistent with the high deprotonation energy of **3**. The decomposition of **3** was studied in detail by collisional activation and compared with that for ionized **2**. Dramatic differences are observed and are a consequence of low barrier processes for fragmentation of decarbonylated **3**.

We are currently exploring the protonation dynamics of a number of diiron complexes in an effort to further characterize their chemistry with emphasis on comparisons to solution results. These studies will undoubtedly provide new insights into these interesting species.

Acknowledgment is made to the donors of the Petroleum Research Fund, Administered by the American Chemical Society, for support of this Research.

Registry No. **2**, 76722-37-7; **3**, 81616-48-0; **10**, 118599-60-3; **13**, 118599-59-0; C_2D_4, 683-73-8; C_2H_2, 74-86-2; acetaldehyde, 75-07-0; *p*-tolualdehyde, 104-87-0; cinnamaldehyde, 104-55-2; acetone, 67-64-1.

Surface Organometallic Chemistry in the Chemical Vapor Deposition of Aluminum Films Using Triisobutylaluminum: β-Hydride and β-Alkyl Elimination Reactions of Surface Alkyl Intermediates

Brian E. Bent,*,† Ralph G. Nuzzo,* and Lawrence H. Dubois*

Contribution from the AT&T Bell Laboratories, Murray Hill, New Jersey 07974.
Received May 20, 1988

Abstract: Thermal decomposition of triisobutylaluminum (TIBA) to deposit aluminum films shows promise as a way to form conductive contacts on silicon-based electronic devices. An important step in the steady-state deposition is the reaction of TIBA with the growing aluminum surface. We have studied this chemistry by reacting TIBA with single-crystal Al(111) and Al(100) surfaces. A combination of effusive molecular beam scattering, thermal desorption spectroscopy, Auger electron spectroscopy, low-energy electron diffraction, high-resolution electron energy loss spectroscopy, and scanning electron microscopy was used in these studies. We find that TIBA decomposes on both of these aluminum surfaces above ~470 K by β-hydride elimination reactions to deposit aluminum and evolve hydrogen and isobutylene. This surface β-hydride elimination reaction is the rate-determining step. We find that the reaction is 2–5 times faster on Al(111) than on Al(100). In the temperature range of 470–600 K, the growing film is carbon-free, crystalline, and adopts the orientation of the single-crystal substrate. At higher temperatures, the deposited aluminum contains carbon, and we present evidence that a surface β-methyl elimination reaction is responsible, at least in part, for this contamination. Using the kinetic parameters determined from monolayer thermal deposition experiments for this reaction, we are able to predict the rate of steady-state aluminum deposition for TIBA pressures between 10^{-6} and 1 Torr.

1. Introduction

Of the many sophisticated technologies currently used in electronic materials growth and processing, perhaps none exhibits a richer, more diverse and perplexing range of chemistries than does chemical vapor deposition (CVD).[1] The many advantages of this technique for growing thin films—enhanced conformal coverage, low processing temperatures to name but a few—are well-appreciated. The current literature, which describes commercially significant processes for the growth of oxide, metal, semiconductor, glass, and compound thin-film materials,[2] attests to the broad range of applications that have been developed. At the heart of all of these technologies reside poorly understood patterns of chemical reactivity, namely the adsorption, activation, and transformation of complex gaseous reagents by a solid surface. This is the central focus of the studies reported here.

The system we examine is aluminum film growth by the pyrolysis of triisobutylaluminum (TIBA). We have selected this system for several reasons. First, it is a process that is of significant current interest for the metalization of very large scale integrated (VLSI) devices with feature sizes less than ~1 μm.[3] Second, the process, as it currently stands, is poorly understood and exhibits complex growth patterns, which may emerge as a direct consequence of fundamental chemical processes occurring on the surface of the substrate.[3,4] Third, and perhaps most significant, this system demonstrates chemical principles that are broadly representative of many CVD systems. As a result, the understanding we develop here may help to suggest approaches by which the relevant features of other systems might be explored.

Scheme I

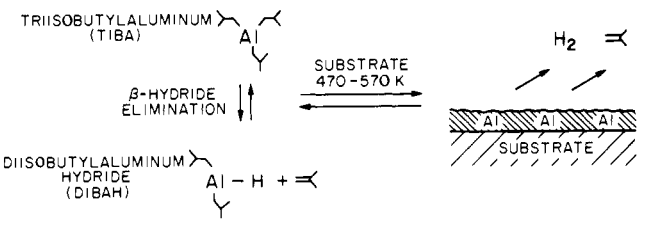

Putting these generalities aside for the moment, it would be useful to discuss specific issues of interest in this aluminum CVD system. Ziegler and co-workers reported in 1960 that triisobutylaluminum can be pyrolyzed at ~525 K to deposit aluminum films.[5] By analysis of the gas-phase products (primarily iso-

† AT&T Bell Laboratories Postdoctoral Fellow. Permanent address: Department of Chemistry, Columbia University, New York, NY 10027.

(1) Sze, S. M. *Semiconductor Devices: Physics and Technology*; Wiley: New York, 1985; Chapter 9, and references therein.
(2) Kern, W.; Ban, V. S. Chemical Vapor Deposition of Inorganic Thin Films. In *Thin Film Processes*; Vossen, J. L., Kern, W., Eds.; Academic Press: New York, 1978; Chapter III-2, and references therein.
(3) Cooke, M. J.; Heinecke, R. A.; Stern, R. C.; Maes, J. W. C. *Solid State Technol.* **1982**, *25*, 62.
(4) Green, M. L.; Levy, R. A.; Nuzzo, R. G.; Coleman, E. *Thin Solid Films* **1984**, *114*, 367. Levy, R. A.; Green, M. L.; Gallagher, P. K. *J. Electrochem. Soc.* **1984**, *131*, 2175.
(5) Ziegler, K.; Nagel, K.; Pfohl, W. *Justus Liebigs Ann. Chem.* **1960**, *629*, 210.

0002-7863/89/1511-1634$01.50/0